Fabrication of Functional Coating Layer for Emerging Transparent Electrodes using Antimony Tin Oxide Nano-colloid

Hoai Han NGUYEN [1], Quang Hai TRAN [1], Young Seok KIM [2], Young-Sang CHO [1] *

[1] *Department of Chemical Engineering and Biotechnology, Tech University of Korea, 237 Sangidaehak-ro, Siheung-si, Gyeonggi-do 15073, Republic of Korea*
[2] *Display Components & Materials Research Center, Technology Institute, 68 Yatap, Bundang, Seongnam-si, Gyeonggi-do, Korea*

http://doi.org/10.5755/j02.ms.34452

Received 29 June 2023; accepted 2 October 2023

This study fabricated a functional coating layer for transparent electrodes using antimony tin oxide nanopowder. The wet grinding method was employed to create a stable dispersion solution of antimony tin oxide nanopowder with aminopropyl tri-methoxysilane and acetyl acetone as primary dispersing agents. Various concentrations of these dispersing agents were used to determine optimal conditions, followed by a gel reaction to form a stable solution. The primary objective was to provide a viable alternative to indium-based transparent electrodes, specifically indium tin oxide, by incorporating antimony oxide. This approach not only addresses limitations associated with indium, but also enhances mechanical properties. The methodology involves the utilization of antimony tin oxide nanopowder and various solvents including ethanol and aforementioned dispersing agents to create a stable antimony tin oxide sol through wet grinding. Effects of dispersant concentration and milling time on the secondary particle size of the antimony tin oxide sol were thoroughly evaluated. Furthermore, this study examined sheet resistance of resulting coating layers by conducting a comparative analysis between antimony tin oxide and indium tin oxide under similar conditions. Findings of this study meticulously detailed in subsequent sections of the manuscript provide valuable insights into optimizing the entire process, encompassing synthesis, coating, heat treatment, and the production of high-quality transparent conductive coatings. These techniques and outcomes can significantly contribute to the development of more sustainable and cost-effective alternatives to traditional indium-based transparent electrodes.

Keywords: antimony tin oxide, spin-coating, transparent electrode, nano-colloid, wet grinding.

1. INTRODUCTION

In recent years, there has been a growing emphasis in industries such as electronics, displays, and solar cells on achieving compact and lightweight designs while incorporating functionalities such as transparency, flexibility, and durability [1 – 4]. The application of indium tin oxide (ITO) thin film transparent conductive coatings through vacuum deposition has been predominantly utilized in touch panel technologies [5 – 10]. ITO thin films possess advantageous properties including high transmittance and excellent electrical conductivity, making them well-suited for deployment as transparent electrode materials in the display industry [11 – 14]. Transparent conducting films can serve as electrodes in electronic and optoelectronic devices, facilitating low-resistance electrical contacts while enabling the transmission of a significant portion of incident light [15 – 17]. These devices encompass liquid-crystal displays (LCDs), flat panel displays, light-emitting diodes (LEDs), and photovoltaic systems [18].

However, the use of indium in ITO coatings presents certain limitations such as high production costs attributed to limited reserves, susceptibility to corrosion when subjected to bending, poor wear resistance, and brittleness [19 – 21]. These drawbacks pose challenges for the application of ITO on plastic substrates with substantial deformation. Consequently, extensive research efforts have been dedicated to exploring alternative materials and seeking substitutes for ITO in transparent conductive coatings. Ongoing investigations aim to identify materials that can offer comparable or superior properties to ITO while addressing its limitations, thereby providing more sustainable and cost-effective solutions for future technological advancements. The primary objective of this study was to investigate the potential of antimony tin oxide (ATO) in conjunction with antimony oxide as a viable substitute for indium-based transparent electrodes, specifically ITO. By incorporating antimony oxide with better extraction levels than indium along with enhanced mechanical properties, this study aimed to develop a next-generation transparent electrode that could effectively replace ITO [22, 23].

Furthermore, considering the projected future demand for transparent electrodes in the widespread deployment of kiosks, our research aimed to establish optimized process parameters for each manufacturing step, including synthesis of a nano-colloidal dispersion, deposition via the spin coating technique, controlled heat treatment, and fabrication of a coating layer with exceptional transparent conductivity. By systematically deriving optimal conditions for these processes, we endeavour to achieve a high-quality coating layer exhibiting superior transparent conductivity, meeting

* Corresponding author. Tel.: +82-31-8041-0612; fax: +82-31-8041-0629. E-mail: *yscho78@tukorea.ac.kr* (Y. S. Cho)

stringent requirements for the production of transparent electrodes in diverse applications. Successful realization of this research holds significant promise for the advancement of transparent electrode technology, offering an alternative to costly and limited indium resources that ITO-based electrodes currently rely on.

2. METHODOLOGY

ATO nano-colloid thin films were fabricated through spin-coating employing ATO nanopowder procured from Sigma-Aldrich. The solvent used for the preparation was ethanol (99.9 %, HPLC grade, Daejung Chemical). Dispersing solvents, namely acetyl acetone (ACAC, 99.0 %, Junsei Chemical Co.) and N-(2-Aminoethyl)-3-aminopropyltri-methoxysilane (AAPTS, Sigma-Aldrich), a silane-based binder with methoxy groups, were utilized in the process. Silane coupling agents with relatively small molecular weights are capable of chemically adsorbing onto ATO particles. Therefore, they are considered a suitable choice for serving as a steric stabilizer in the ATO coating solution to achieve a stable colloidal ATO solution. Acetylacetone is widely recognized as a bidentate ligand that exhibits the ability to attach to the surface of metal oxide particles, effectively preventing their aggregation. Due to the inherent tendency of ATO powder to aggregate when exposed to organic solvents, it becomes necessary to disperse agglomerated ATO particles through the application of collision energy in conjunction with a steric stabilizer [24 – 26]. To accomplish this, various types of milling machines can be employed. In laboratory settings, a batch-type vibratory milling machine, such as a paint shaker, has been proven to be the most suitable option. Within the paint shaker, aggregated ATO particles undergo collision with beads, resulting in their fragmentation. By utilizing this equipment, a stable ATO sol can be obtained within a relatively short milling duration of several hours.

Dispersing agents employed in this investigation, namely AAPTS and ACAC, were solubilized in 10 mL of ethanol with specific concentrations specified in Table 1.

Table 1. A detailed description of the colloidal solution

Sample type	Dispersants	Milling time, hour	Spin speed, rpm
ATO	AAPTS 0.2M	2/4/6	2500 rpm
ATO	AAPTS 0.2M	2/4/6	3500 rpm
ATO	AAPTS 0.2M	2/4/6	4500 rpm
ATO	AAPTS 0.4M	2/4/6	2500 rpm
ATO	AAPTS 0.8M	2/4/6	2500 rpm
ATO	ACAC 0.2M	2/4/6	2500 rpm
ITO	AAPTS 0.2M	2/4/6	2500 rpm
ITO	ACAC 0.2M	2/4/6	2500 rpm

To ensure the formation of a homogeneous solution, the mixture was stirred using a magnetic stirrer for one hour. Subsequently, 0.8 g of ATO powder was introduced into the solution to produce a solution with spatial stability. A polypropylene Nalgen bottle of 12.5 mL was utilized for containing the ATO sol. To reduce the secondary particle sizes of ATO particles, zirconia beads (3 mL, diameter of 0.3 mm) were added to the ATO suspension, which underwent milling via a vibratory milling machine. This procedure is shown schematically in Fig. 1 a and b. In this study, ITO was also included in the experimental procedure following a similar process as ATO, aiming to facilitate a comparative analysis.

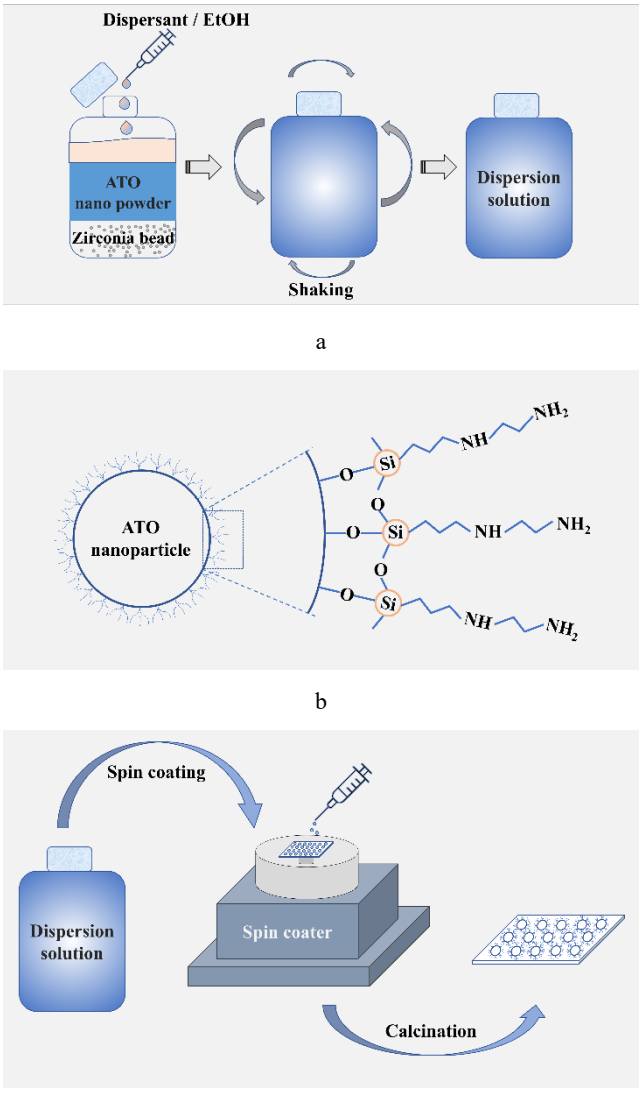

Fig. 1. a – schematic view of the wet grinding method using a paint shake; b – schematic figure for surface-modified ATO nanoparticles after wet attrition process using AAPTS as dispersing agent; c – production of a colloidal film using the spin-coating technique

As illustrated in Fig. 1 c, dispersions were subsequently applied onto a glass substrate using the spin-coating technique, employing speeds ranging from 2500 to 4500 rpm for 30 seconds. Before the spin-coating process, glass substrates (2.5 cm × 2.5 cm × 0.2 cm) underwent a comprehensive cleaning procedure. Initial cleaning involved washing substrates with a detergent solution, followed by ultrasonic cleaning in acetone, methanol, and isopropanol for 15 minutes each. Prepared dispersion solutions were then applied to the glass substrate using Jaesung Engineering's Spin Coater JS301, with a coating volume of 250 µL. Subsequently, heat treatment was conducted for 5 hours at 550 °C after applying each coating film. Silver paste (CANS ELCOAT P-100) was used to measure the resistance to create five electrode patterns with equal intervals of 5 mm and a line width of 1 mm as shown

in Fig. 2 a. Resistance measurements were performed after allowing ample drying time at room temperature for one day. The first electrode was contacted with a probe. The resistance was measured by moving the other search sequentially from the second electrode to the fifth electrode.

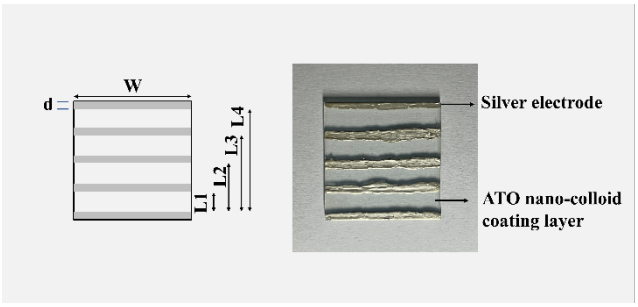

a

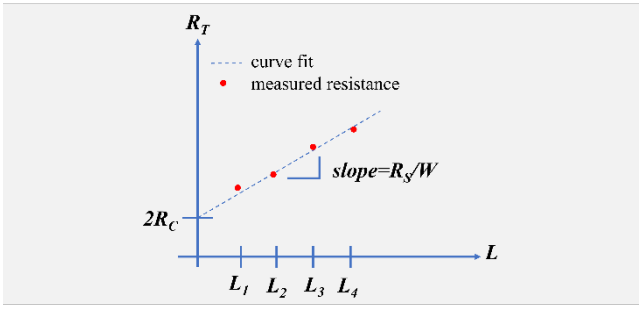

b

Fig. 2. a – a transmission line method test structure (left), and a photographic image of the actual sample (right); b – plots of total resistance versus contact spacing for explaining the TLM measurement technique

Various methods exist for measuring Ohmic contacts at the metal/semiconductor interface. Of them, the transmission line model (TLM) is commonly employed to assess contact resistance. The total measured resistance encompasses multiple components given by the following equation:

$$R_T = 2R_m + 2R_C + R_{semi}, \quad (1)$$

where R_m is the resistance attributed to the contact metal; R_C is associated with the metal/semiconductor interface; R_{semi} denotes the typical semiconductor resistance. The resistance of an individual contact is represented by $R_m + R_C$. However, in most cases, the metal's resistivity in the contact is significantly lower than R_C, making R_m negligible.

Resistance of the semiconductor can be expressed as

$$R_{semi} = R_S \times L/W, \quad (2)$$

where R_S is the sheet resistance; L is the length; W is the width of the semiconductor region. The total resistance, R_T, can be defined as

$$R_T = R_S/W \times L + 2R_C, \quad (3)$$

taking into account the contribution of the semiconductor resistance and the metal/semiconductor interface resistance. By constructing resistors with varying lengths while keeping all other parameters constant, the total resistances of each resistor can be measured and plotted. In the case of a resistor with zero length, the remaining resistance is precisely twice the contact resistance. This contact resistance value can be determined by extrapolating from the graph back to $L = 0$. Additionally, the slope of the line provides information about the sheet resistance of the semiconductor, which is an additional benefit of this measurement technique [27].

To facilitate the measurement process, a typical configuration for the TLM test pattern is depicted in Fig. 2 a. The pattern included an array of contacts (depicted in darker gray) with different spacings, positioned over the doped region. In this specific experiment, TLM patterns employed a width (W) of 25 mm and different lengths (L) of 5 mm, 11 mm, 17 mm, and 23 mm. Resistance measurements between each pair of contacts were used to construct the TLM graph as shown in Fig. 2 b. From the graph, the RS parameter representing sheet resistance can be determined and recorded for further analysis.

3. RESULTS AND DISCUSSION

Fig. 3 depicts transmission spectra measured using a visible UV spectrophotometer for samples before and after heat treatment. It was evident that heat-treated samples exhibited a significant increase in transparency of the ATO coating, reaching approximately 90 % in the 500 ~ 550 nm wavelength compared to untreated samples. The transmission intensity showed a slight upward trend as the spin-coating speed increased, indicating a reduction in the thickness of the coating layer. However, an excessively thin coating also affected the distribution of ATO particles on glass substrates. In this study, a spinning speed of 2500 rpm was considered suitable for creating a uniform ATO adhesive coating on glass substrates.

Fig. 4 a illustrates the impact of dispersant concentration and milling time on the secondary particle size of the ATO solution. The dispersant used in this study was AAPTS at different concentrations of 0.1M, 0.2M, 0.4M, and 0.8M. The grinding process was conducted for 2 hours, 4 hours, and 6 hours, respectively. We could clearly observe a trend where the size of secondary particles decreased as the concentration of the dispersant AAPTS increased from 0.1M to 0.2M. As the dispersant concentration increased, the number of grafted AAPTS per unit ITO surface area increased. Therefore, the repulsive force between particles also increased, resulting in a more dispersed distribution of particles. However, if the dispersant concentration was too high (specifically at 0.4M and 0.8M), the interparticle repulsive force became chaotic, causing particles to agglomerate.

ACAC is present in two forms: keto form and enol form, with the enol form accounting for about 76 % of the total. The enol form is more stable due to resonance stabilization of conjugated double bonds and hydrogen bonding. As hydroxyl groups in the enol form are highly reactive, they can adsorb and form chelation with the ATO surface. This coordinated compound of acetylacetone on the ATO surface creates a steric barrier that can prevent van der Waals attraction, thus stabilizing the dispersion of the ATO sol [28]. In Fig. 4 b, ACAC and AAPTS were used as stabilizing agents for the comparative experiment between ATO and ITO. Results demonstrated that, with a dispersant concentration of 0.2M, the size of secondary particles after 6 hours of milling was nearly the same.

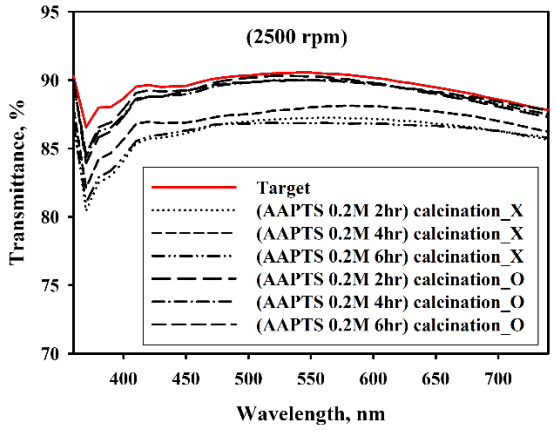

a

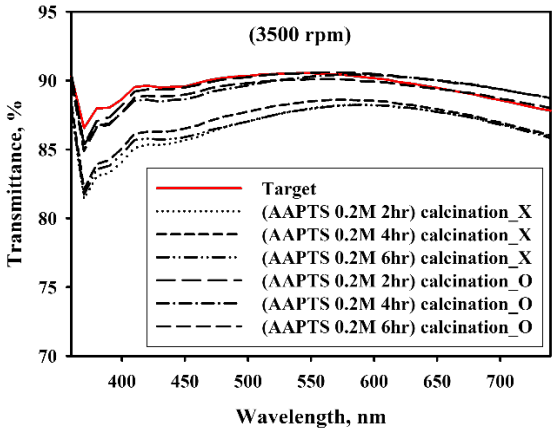

b

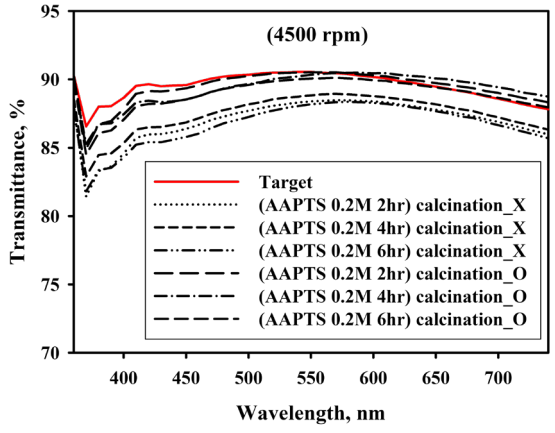

c

Fig. 3. Transmittance spectra of ATO thin films prepared with different spin speed (2500, 3500, 4500 rpm)

However, there was a distinct difference in the size of secondary particles between ATO and ITO, measuring approximately 166 nm and 110 nm, respectively, after 6 hours of milling.

Fig. 5 illustrates results of the sheet resistance for coating layers. The sheet resistance of coating layers using AAPTS dispersant at concentrations of 0.4M and 0.8M was nearly indeterminable. Results of sheet resistance of coating layers using AAPTS dispersant at concentrations of 0.1M and 0.2M are shown in Fig. 5 a. Based on the graph, it could be observed that increasing the APTS concentration from 0.1M to 0.2M and increasing the milling time from 2 hours to 6 hours resulted in a reduction in the size of ATO secondary particles.

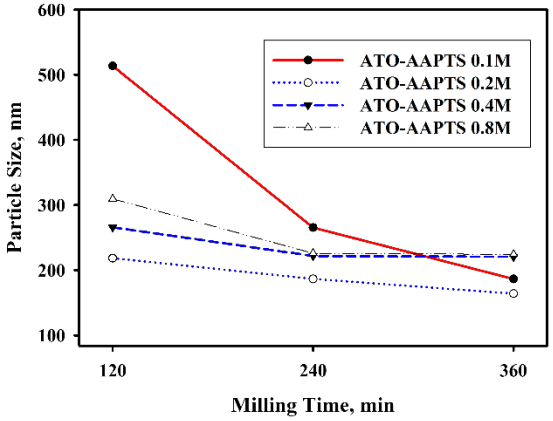

a

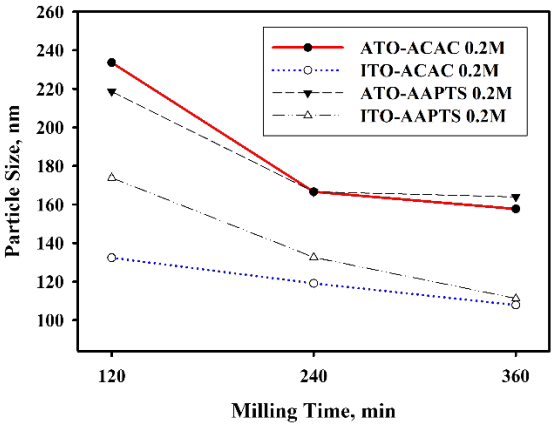

b

Fig. 4. Secondary particle size of ATO and ITO with milling time

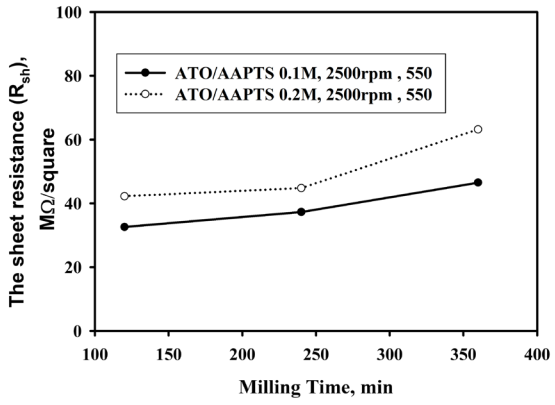

a

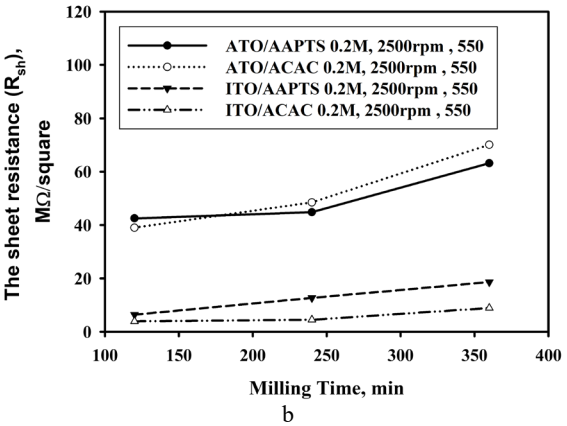

b

Fig. 5. Sheet resistance of ATO and ITO films spin-coated at 2500 rpm using ACAC and AAPTS as dispersing agents

The decrease in the size of secondary particles in the coating solution led to an increase in the sheet resistance of the coating due to an increased contact resistance between ATO aggregates. However, according to comparison results between ATO and ITO shown in Fig. 5 b, despite a significantly smaller size of secondary ITO particles after 6 hours of milling compared to secondary ATO particles, the sheet resistance of the coating using ITO was still lower than that of the coating using ATO. This indicated that although ATO could be utilized to create functional coating layers for electrodes, in terms of performance, ITO still demonstrated better electrical conductivity results.

4. CONCLUSIONS

In this study, dispersion of nano ATO powder was achieved under stable conditions using the wet milling method followed by spin-coating to create a coating layer. Subsequently, a heat treatment process was conducted at 550 °C for 5 hours to reduce surface resistance. Finally, conditions were evaluated by measuring physical properties such as transmittance, secondary particle size analysis, and sheet resistance. Under the same milling conditions, the ATO sol was stabilized by dispersing agents APPTS and ACAC. The sheet resistance of the coating layers was determined using the transmission line method (TLM).

Under the most stable conditions, the sheet resistance of the coating layer using the ATO sol after 6 hours of milling was measured to be 61.17 MΩ/□ for APTS and 70.1 MΩ/□ for ACAC. Under the same experimental conditions, the sheet resistance of the coating layer using the ITO sol resulted in values of 18.6 MΩ/□ for APTS and 8.9 MΩ/□ for ACAC. Despite its limitations compared to ITO, the use of ATO as a substitute material for transparent conductive coatings has been demonstrated in this study. Successful completion of this research offers a potential solution for substituting expensive materials in the future.

Acknowledgments

This research was supported by Priority Research Centers Program through the National Research Foundation of Korea (NRF) funded by the Ministry of Education (NRF-2017R1A6A1A03015562) and the National Research Foundation of Korea (NRF) grant funded by the Korea government (MSIT) (No. 2021R1F1A1047451 and No. RS-2023-00250648).

REFERENCES

1. **Lu, S., Sun, Y., Ren, K., Liu, K., Wang, Z., Qu, S.** Recent Development in ITO-free Flexible Polymer Solar Cells *Polymers* 10 (1) 2018: pp. 5. https://doi.org/10.3390/polym10010005
2. **Morales-Masis, M., Wolf, S.D., Woods-Robinson, R., Ager, J.W., Ballif, C.** Transparent Electrodes for Efficient Optoelectronics *Advanced Electronic Materials* 3 (5) 2017: pp. 1600259. https://doi.org/10.1002/aelm.201600529
3. **Sannicolo, T., Lagrange, M., Cabos, A., Celle, C., Simonato, J.P., Bellet, D.** Metallic Nanowire-Based Transparent Electrodes for Next Generation Flexible Devices: a Review *Small Journal* 12 (44) 2016: pp. 6052 – 6075. https://doi.org/10.1002/smll.201602581
4. **Nathan, A., Ahnood, A., Cole, M.T., Lee, S., Suzuki, Y., Hiralal, P., Bonaccorso, F., Hasan, T., Garcia-Gancedo, L., Dyadyusha, A., Haque, S., Andrew, P., Hofmann, S., Moultrie, J., Chu, D., Flewitt, A.J., Ferrari, A.C., Kelly, M.J., Robertson, J., Amaratunga, G.A.J., Milne, W.I.** Flexible Electronics: The Next Ubiquitous Platform *Proceedings of the IEEE* 100 2012: pp. 1486 – 1517. https://doi.org/10.1109/JPROC.2012.2190168
5. **Txintxurreta, J., Berasategui, E.G., Ortiz, R., Hernández, O., Mendizábal, L., Barriga, J.** Indium Tin Oxide Thin Film Deposition by Magnetron Sputtering at Room Temperature for the Manufacturing of Efficient Transparent Heaters *Coatings* 11 (1) 2021: pp. 92. https://doi.org/10.3390/coatings11010092
6. **Chiang, J.L., Li, S.W., Yadlapalli, B.K., Wuu, D.S.** Deposition of High-transmittance ITO Thin Films on Polycarbonate Substrates for Capacitive-touch Applications *Vacuum* 186 2021: pp. 110046. https://doi.org/10.1016/j.vacuum.2021.110046
7. **Tran, D.P., Lu, H.I., Lin, C.K.** Conductive Characteristics of Indium Tin Oxide Thin Film on Polymeric Substrate under Long-Term Static Deformation *Coatings* 8 (6) 2018: pp. 212. https://doi.org/10.3390/coatings8060212
8. **Sezemsky, P., Burnat, D., Kratochvil, J., Wulff, H., Kruth, A., Lechowicz, K., Janik, M., Bogdanowicz, R., Cada, M., Hubicka, Z., Niedziałkowski, P., Białobrzeska, W., Stranak, V., Śmietana, M.** Tailoring Properties of Indium Tin Oxide Thin Films for Their Work in Both Electrochemical and Optical Label-free Sensing Systems *Sensors and Actuators B: Chemical* 343 2021: pp. 130173. https://doi.org/10.1016/j.snb.2021.130173
9. **Ramanauskas, R., Iljinas, A., Marcinauskas, L., Milieška, M., Kavaliauskas, Ž., Gecevičius, G., Čapas, V.** Deposition and Application of Indium-Tin-Oxide Films for Defrosting Windscreens *Coatings* 12 (5) 2022: pp. 670. https://doi.org/10.3390/coatings12050670
10. **Heffner, H., Soldera, M., Lasagni, A.F.** Optoelectronic Performance of Indium Tin Oxide Thin Films Structured by Sub-picosecond Direct Laser Interference Patterning *Scientific Reports* 13 (1) 2023: pp. 9798. https://doi.org/10.1038/s41598-023-37042-y
11. **Park, G.B., Kim, D.B., Kim, G.W., Jeong, U.Y.** High-Performance Indium-Tin Oxide (ITO) Electrode Enabled by a Counteranion-Free Metal-Polymer Complex *ACS Nanosci Au* 2 (6) 2022: pp. 527 – 538. https://doi.org/10.1021/acsnanoscienceau.2c00027
12. **Wahab, O.J., Kang, M., Meloni, G.N., Daviddi, E., Unwin, P.R.** Nanoscale Visualization of Electrochemical Activity at Indium Tin Oxide Electrodes *Analytical Chemistry* 94 (11) 2022: pp. 4729 – 4736. https://doi.org/10.1021/acs.analchem.1c05168
13. **Dalapati, G.K., Sharma, H., Guchhait, A., Chakrabarty, N., Bamola, P., Liu, Q., Saianand, G., Krishna, A.M.S., Mukhopadhyay, S., Dey, A., Wong, T.K.S., Zhuk, S., Ghosh, S., Chakrabortty, S., Mahata, C., Biring, S., Kumar, A., Ribeiro, C.S., Ramakrishna, S., Chakraborty, A.K., Krishnamurthy, S., Sonar, P., Sharma, M.** Tin Oxide for Optoelectronic, Photovoltaic and Energy Storage Devices: A Review *Journal of Materials Chemistry A* 9 2021: pp. 16621 – 16684. https://doi.org/10.1039/D1TA01291F

14. **Ma, Z., Li, Z., Nouri, B.M., Liu, K., Ye, C., Dalir, H., Sorger, V.J.** Indium-Tin-Oxide for High-performance Electro-optic Modulation *Applied Physics* 2305.10639 2023: pp. 1 – 16. https://doi.org/10.48550/arXiv.2305.10639

15. **Cao, W., Li, J., Chen, H., Xue, J.** Transparent Electrodes for Organic Optoelectronic Devices: A Review *Journal of Photonics for Energy* 4 (1) 2014: pp. 040990. https://doi.org/10.1117/1.JPE.4.040990

16. **Singha, S., Sharmaa, V., Asokanc, K., Sachdev, K.** NTO/Ag/NTO Multilayer Transparent Conducting Electrodes for Photovoltaic Applications Tuned by Low Energy Ion Implantation *Solar Energy* 173 2018: pp. 651 – 664. https://doi.org/10.1016/j.solener.2018.08.001

17. **Catrysse, P.B., Fan, S.** Nanopatterned Metallic Films for Use As Transparent Conductive Electrodes in Optoelectronic Devices *Nano Letters* 10 (8) 2010: pp. 2944 – 2949. https://doi.org/10.1021/nl1011239

18. **Kim, H.K., Lee, S.G., Yun, K.S.** Capacitive Tactile Sensor Array for Touch Screen Application *Sensors and Actuators A: Physical* 165 (1) 2011: pp. 2 – 7. https://doi.org/10.1016/j.sna.2009.12.031

19. **Gwamuri, J., Vora, A., Khanal, R.R., Phillips, A.B., Heben, M.J., Guney, D.O., Bergstrom, P., Kulkarni, A., Pearce, J.M.** Limitations of Ultra-thin Transparent Conducting Oxides for Integration into Plasmonic-enhanced Thin-film Solar Photovoltaic Devices *Materials for Renewable and Sustainable Energy* 4 (12) 2015: pp. 1 – 11. https://doi.org/10.1007/s40243-015-0055-8

20. **Hamasha, M.M., Alzoubi, K., Lu, S., Desu, S.B.** Durability Study on Sputtered Indium Tin Oxide Thin Film on Poly Ethylene Terephthalate Substrate *Thin Solid Films* 519 (18) 2011: pp. 6033 – 6038. https://doi.org/10.1143/JJAP.38.2856

21. **Hsu, J.S., Lee, C.C., Wen, B.J., Huang, P.C., Xie, C.K.** Experimental and Simulated Investigations of Thin Polymer Substrates with an Indium Tin Oxide Coating under Fatigue Bending Loadings *Materials* 9 (9) 2016: pp. 720. https://doi.org/10.3390/ma9090720

22. **Nguyen, C.K., Low, M.X., Zavabeti, A., Murdoch, B.J., Guo, X., Aukarasereenont, P., Mazumder, A., Dubey, A., Jannat, A., Rahman, M.A., Chiang, K., Truong, V.K., Bao, L., McConville, C.F., Walia, S., Daeneke, T., Syed, N.** Atomically Thin Antimony-Doped Indium Oxide Nanosheets for Optoelectronics *Advanced Optical Materials* 10 (20) 2022: pp. 2200925. https://doi.org/10.1002/adom.202200925

23. **Liu, C., Félix, R., Forberich, K., Du, X., Heumüller, T., Matt, G.J., Gu, E., Wortmann, J., Zhao, Y., Cao, Y., He, Y., Ying, L., Hauser, A., Oszajca, M.F., Hartmeier, B.** Utilizing the Unique Charge Extraction Properties of Antimony Tin Oxide Nanoparticles for Efficient and Stable Organic Photovoltaics *Nano Energy* 99 (A) 2021: pp. 106373. https://doi.org/10.1016/j.nanoen.2021.106373

24. **Kooa, B.R., Baeb, J.W., Ahn, H.J.** Low-temperature Conducting Performance of Transparent Indium Tin oxide/antimony Tin Oxide Electrodes *Ceramics International* 43(8) 2017: pp. 6124 – 6129. https://doi.org/10.1016/j.ceramint.2017.02.006

25. **Peyre, V., Spalla, O., Belloni, L.** Compression and Reswelling of Nanometric Zirconia Dispersions: Effect of Surface Complexants *Journal of the American Ceramic Society* 82 (5) 2004: pp. 1121 – 1128. https://doi.org/10.1111/j.1151-2916.1999.tb01885.x

26. **Almansoori, Z., Khorshidi, B., Sadri, B., Sadrzadeh, M.** Parametric Study on the Stabilization of Metal Oxide Nanoparticles in Organic Solvents: A Case Study with Indium Tin Oxide (ITO) and Heptane *Ultrasonics Sonochemistry* 40 (part A) 2018: pp. 1003 – 1013. https://doi.org/10.1016/j.ultsonch.2017.09.012

27. **Grover, S., Sahu, S., Zhang, P., Davis, K.O., Kurinec, S.K.** Standardization of Specific Contact Resistivity Measurements using Transmission Line Model (TLM) *International Conference on Microelectronic Test Structures* 33 2020: pp. 1 – 6. https://doi.org/10.1109/ICMTS48187.2020.9107911

28. **Connor, P.A., Dobson, K.D., McQuillan, A.J.** New Sol-Gel Attenuated Total Reflection Infrared Spectroscopic Method for Analysis of Adsorption at Metal Oxide Surfaces in Aqueous Solutions. Chelation of TiO_2, ZrO_2, and Al_2O_3 Surfaces by Catechol, 8-Quinolinol, and Acetylacetone *Langmuir* 11 (11) 1995: pp. 4193 – 4195. https://doi.org/10.1143/JJAP.38.2856